*30th EPS Conference on Contr. Fusion and Plasma Phys., St. Petersburg, 7-11 July 2003 ECA Vol. **27A**, P-1.136*

Z_{eff} Behaviour in ASDEX Upgrade H-mode Discharges

H. Meister, L. D. Horton, B. Kurzan, W. Suttrop, H. Zohm and ASDEX Upgrade Team

Max-Planck-Institut für Plasmaphysik, EURATOM Assoziation
Boltzmannstr. 2, D-85748 Garching b. München

Introduction The characterisation of the impurity content of a fusion plasma is still an important task as the performance of future burning plasma experiments like ITER will degrade with increasing impurity content. A commonly used quantity characterising the impurity content is the effective charge state $Z_{\mathrm{eff}} = \sum_i n_i Z_i^2 / \sum_i n_i Z_i$ which can be derived e. g. from absolutely calibrated measurements of bremsstrahlung when the radial profiles of electron density n_e and temperature T_e are known. As a weighted average, Z_{eff} will be dominated by the contribution of low Z impurities; impurities such as W give in ASDEX Upgrade a $\Delta Z_{\mathrm{eff}} \leq 0.3$.

Usually, the measurement of bremsstrahlung is carried out by recording the plasma emission in a certain wavelength range free of line radiation using interference filters and varying types of diodes as detectors. Mostly, a narrow band in the green range of the spectrum is used. The range of up to $5\,nm$ around $537\,nm$ is reported to be line free in several machines. At ASDEX Upgrade, the existing filter/detector combinations of the vertical Thomson scattering diagnostic (VTS) [1] were mainly used for bremsstrahlung measurements. Although the sensitive Avalanche-diodes used as detectors are very well suited to measure the low intensities of the bremsstrahlung, the interference filters are not optimised for this task. They observe rather broad spectral ranges (up to $80\,nm$) in the near infrared region. Therefore, the bremsstrahlung signals may be disturbed by line radiation and/or thermal radiation from hot parts of the plasma facing components. To compensate for these disadvantages a new approach has been devised to determine Z_{eff} from bremsstrahlung measurements. A new diagnostic set-up was brought into operation which measures the bremsstrahlung emission spectrally resolved. In order to take advantage of the strengths of the various measurements and to provide checks for signal contamination, all available signals measuring bremsstrahlung have been included in one evaluation procedure to deduce one consistent Z_{eff} profile.

Current diagnostic set-up and data evaluation At ASDEX Upgrade bremsstrahlung emission from the plasma is measured along many lines-of-sight. These are shown in figure 1, mapped onto a poloidal cross-section. As they were optimised for different purposes, they differ in the type of their detectors, temporal resolution, sensitivity and wavelength range of observation. As mentioned above, the bremsstrahlung measured with the sight-lines from VTS frequently suffer from line and/or thermal radiation due to the broad interference filters in the near infrared. The sight-lines of diagnostic ZEA are equipped with an interference filter in the green spectral range ($5\,nm$ wide, centred at $538\,nm$) and a diode array as detector. No thermal and almost no line radiation is observed by this diagnostic, but the rather insensitive diode-array results in a poor signal-to-noise ratio and its data is therefore not useful for Z_{eff} profile evaluation. Nonetheless these sight-lines provide a good check for data consistency of diagnostic VTS.

The diagnostic ZEB was recently constructed to complement the information on bremsstrahlung emissivity of the plasma from the other two diagnostics discussed above. Its 12 sight-lines view the plasma edge at the outer mid-plane in a toroidal cross-section. Another two sight-lines are used to monitor the plasma centre. The plasma emission is detected using a

Czerny-Turner type spectrograph and a back-illuminated frame-transfer CCD-camera, leading to a good separation of line radiation and bremsstrahlung. For the determination of Z_{eff}, the wavelength range between 532–562 nm is usually used at a cycle time of 60 ms, which gives a good trade-off with respect to the signal-to-noise ratio.

A new feature is the inclusion of the bremsstrahlung, as measured by the charge exchange recombination spectroscopy (CXRS), in the deconvolution algorithm. As the sight-lines of the CXRS are oriented tangentially in the outer mid-plane and cover the whole minor radius, they may be used to replace the ones of the VTS and thus help avoiding problems due to line and/or thermal radiation. The intensity calibrations of the CXRS and ZEB diagnostic have been refined by using dedicated plasma sweeps accross the sight-lines in order to improve the relative channel-to-channel calibration. The absolute calibration is then fixed in high-density discharges with very low impurity content ($Z_{\mathrm{eff}} \leq 1.5$). For the deconvolution of Z_{eff} profiles from bremsstrahlung measurements, the profiles of n_e and T_e have to be known. They are usually taken from the evaluation of the Thomson-scattering diagnostic. Further more, calculations of the effective Gaunt-factor have to be performed. At ASDEX Upgrade the formulas given in [2] are used to calculate a tabulated data set, from which the Gaunt-factors can be retrieved very efficiently during data evaluation using spline interpolation. As the Gaunt-factors depend on the charge, the deconvolution of Z_{eff} is iterated until the Gaunt-factors do not change any more.

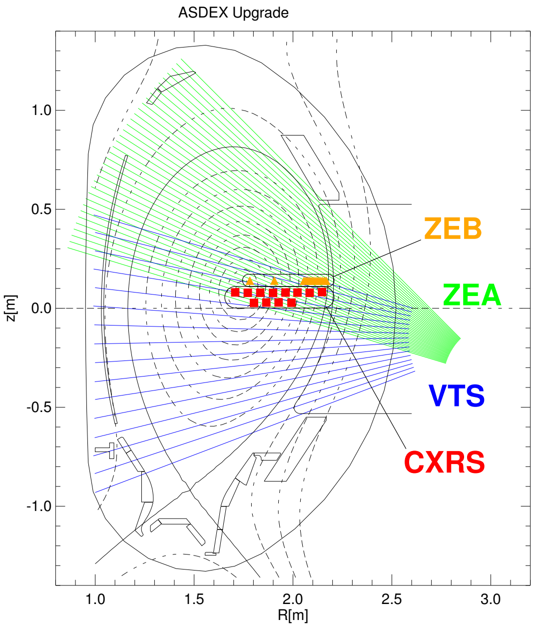

Figure 1: *Sight-lines at ASDEX Upgrade measuring bremsstrahlung emission, mapped into a poloidal cross-section.*

The algorithm adopted for the deconvolution of the bremsstrahlung emissivity, is based on the matrix inversion method and uses curvature minimisation as regularization. The functional, which is minimised, is an extension of the functional of the weighted χ^2-fit to the linear model $\vec{y} = \mathbf{X} \cdot \vec{\beta}$, which is given by $\chi^2 = (\vec{y} - \mathbf{X} \cdot \vec{\beta})^T \cdot \mathbf{W} \cdot (\vec{y} - \mathbf{X} \cdot \vec{\beta})$. A detailed description of its principle and implementation can be found in [3].

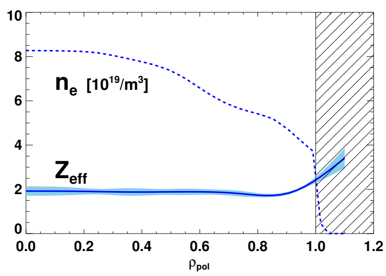

Figure 2: *Z_{eff} profile for an ELMy H-mode discharge at ASDEX Upgrade (#17481, $t = 2.88\,s$).*

During most discharges at least one of the sight-lines from ZEB passes completely outside the separatrix. Despite n_e being very low in this region, a considerable level of emission is measured, which originates mainly from line radiation and radiation from molecular bands resulting in a quasi-continuum. For Z_{eff} profile deconvolution this emission is therefore considered as the emission of a radiative mantle as in [4] and routinely subtracted from the measurements of the remaining sight-lines, resulting in a reduced statistical error of the deconvolved profile.

Z_{eff} in ELMy H-mode discharges In ELMy H-mode discharges at ASDEX Upgrade Z_{eff} profiles are typically flat. An example is shown in figure 2. The region outside the separatrix is shaded because there is no dedicated information on $Z_{\rm eff}$ from outside $\rho_{\rm pol} = 1$. In this case due to being the region whose emission is considered as the radiative mantle. In other cases shown also due to the lack of measurements.

Using the deconvolved $Z_{\rm eff}$ profiles from many discharges, the dependency of the line averaged $Z_{\rm eff}$ values on the plasma density was investigated. As shown in figure 3, $Z_{\rm eff}$ decreases with increasing density. ELMy H-modes achieved during various scenarios with co-injection of neutral beam heating (co-NBI) can be fitted by $Z_{\rm eff} - 1 = \frac{11.2}{n_e - 0.74}$ (figure 3(a)).

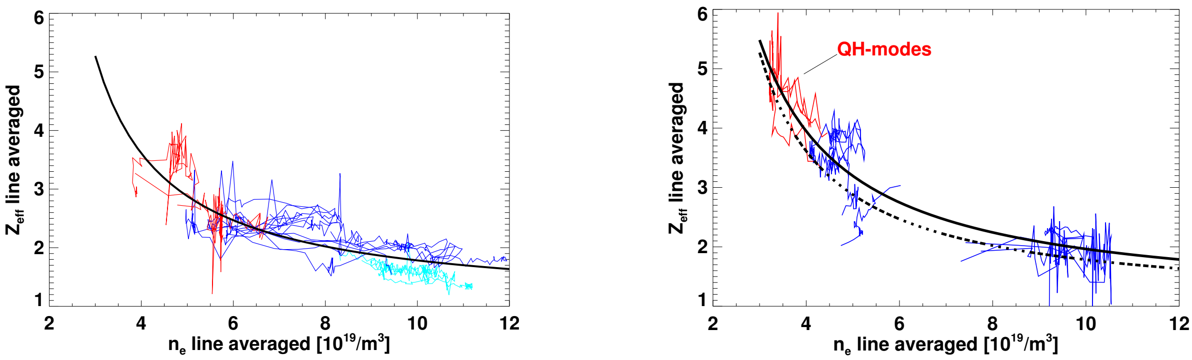

(a) Co-NBI

(b) Ctr-NBI

Figure 3: *Line-averaged Z_{eff} vs. line-averaged density for ELMy H-mode discharges at ASDEX Upgrade*

A similar behaviour is observed for ELMy H-modes during ctr-NBI (figure 3(b)). The same trend can be observed, which applies not only to ELMy H-modes (shown in blue) but also to QH-mode discharges (shown in red). These quiescent H-modes are an ELM-free regime where the transport across the separatrix is taken over by a continuous MHD activity localised at the plasma edge without bursting energy and particle output [5]. In this picture, the relatively high values of $Z_{\rm eff}$ are caused by the low electron densities rather than being a particular feature of QH-modes. H-modes and QH-modes can be fitted by $Z_{\rm eff} - 1 = \frac{12.2}{n_e - 0.96}$. In comparison to the co-NBI case (dotted line), $Z_{\rm eff}$ is somewhat higher.

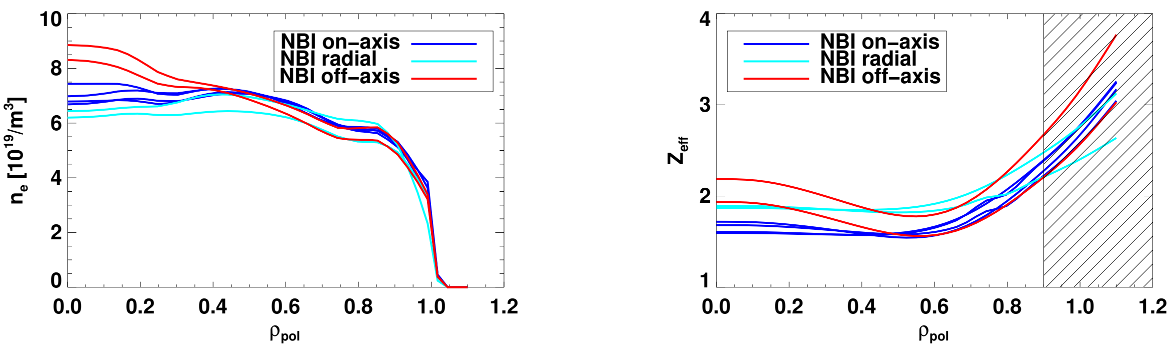

(a) n_e profiles

(b) $Z_{\rm eff}$ profiles

Figure 4: *n_e and Z_{eff} profiles from different time-slices during an H-mode discharge while scanning through all 8 NBI sources at ASDEX Upgrade (#15715).*

At ASDEX Upgrade it has been discovered that the density profile shape can be controlled via the heating power deposition. As shown in [6], a power deposition on-axis leads to flat n_e profiles whereas off-axis power deposition results in peaked n_e profile shapes. For the case of NBI heating this is shown in figure 4(a). The present understanding of this behaviour is based on the assumption that the particle transport is coupled to the energy transport ($D \propto \chi$). The off-axis heating leads to very low values of χ in the plasma centre. According to the assumed proportionality, a pinch of the order of the neoclassical Ware pinch is is now no longer masked and leads to peaked n_e profiles. With peaked $n_e(\rho)$ a neoclassical pinch should lead to increased impurity influx and thus to peaked $Z_{\mathrm{eff}}(\rho)$. For NBI heating this is actually observed as shown in figure 4(b). Using ICRH instead of NBI heating power, $n_e(\rho)$ still shows the expected peaking during time (figure 5(a)). $Z_{\mathrm{eff}}(\rho)$ on the other hand is essentially flat at all time points (figure 5(b)). The different levels of Z_{eff} are only due to different levels of n_e in the respective discharges.

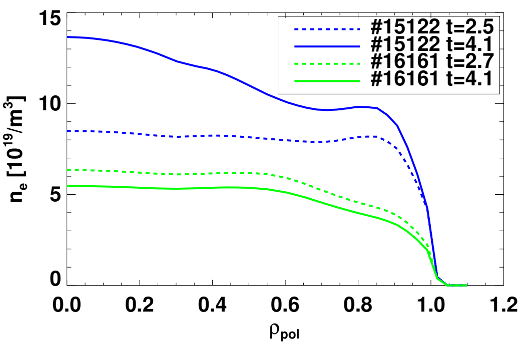

(a) n_e profiles

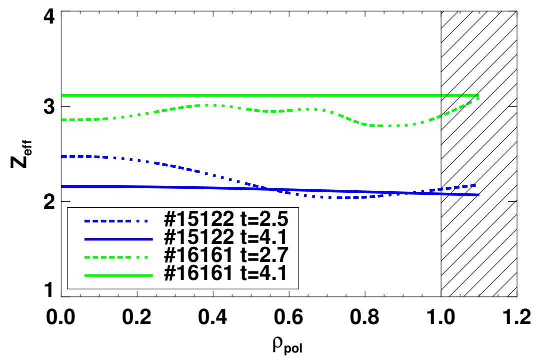

(b) Z_{eff} profiles

Figure 5: *n_e and Z_{eff} profiles during H-mode discharges with on-axis (#16161) and off-axis (#15122) ICRH deposition.*

The reason why NBI and ICRH heated discharges behave differently with respect to the impurity content is still unclear. Further investigations will be done using the improved diagnostical capabilities provided by the inclusion of bremsstrahlung data as well as impurity concentrations from the charge exchange recombination spectroscopy.

References

[1] H. Murmann *et al.*, Review of Scientific Instruments **63**, 4941 (1992).
[2] W. J. Karzas and R. Latter, Astrophysical Journal — Supplement Series **6**, 167 (1961).
[3] H. Meister *et al.*, accepted for publication in Review of Scientific Instruments (2003).
[4] D. G. Whyte *et al.*, Nuclear Fusion **38**, 387 (1997).
[5] W. Suttrop *et al.*, accepted for publication in Plasma Physics and Controlled Fusion (2003).
[6] J. Stober *et al.*, Nuclear Fusion **41**, 1535 (2001).